Non-singular Green's functions for quadratic-order indirect-BEM discretizations: implementation and numerical results

Iago Cavalcante[1], Edivaldo Romanini[2], Josué Labaki[1], Euclides Mesquita[1]

[1]*School of Mechanical Engineering, University of Campinas - Unicamp*
200 Mendeleyev St, 13083-970, Campinas SP Brazil
i209496@dac.unicamp.br, labaki@unicamp.br, euclides@fem.unicamp.br
[2]*Federal University of South Mato Grosso - UFMS*
3484 Ranulpho Marques Leal Av, 79620-080, Tres Lagoas MS Brazil
romanini@ceul.ufms.br

Abstract. This article presents original Green's functions that can used to model bounded and unbounded problems through boundary discretization and meshless methods. Time-harmonic loads are applied within rectangular patches within isotropic, three-dimensional full-spaces. The coupled differential equations describing the problem are solved with the aid of double Fourier transforms. A boundary-value problem corresponding to horizontal and vertical loads with bi-quadratic distribution over the loaded area is considered. The final stress and displacement fields are expressed in terms of double Fourier integrals to be evaluated numerically. These non-singular Green's functions can be thought of as bi-quadratic boundary elements, to be used within direct and indirect boundary element formulations.

Keywords: Boundary Elements Method, Green's functions, Fourier transforms, Numerical integration

1 Introduction

Influence functions are solutions for linear differential equations and a fundamental part of some numerical methods, particularly those based on boundary integral equation discretizations. Influence functions, of which Green's functions are a particular case corresponding to point loads, have been used to model a variety of problems in elastodynamics, such as buried pile groups [1], crack propagation [2], and composites [3]. Analyses of a certain medium through boundary element formulations require the corresponding influence function for that medium to be available or derived.

An example of such influence function, corresponding to 3D full-spaces under uniformly distributed time-harmonic loads, has been introduced by the authors of this article [4–7]. Those displacement and stress solutions may be used in boundary element formulations using constant or linear elements, or superposition schemes considering spatially-constant load distribution [8]. However, constant or linear element discretizations typically require a large number of elements to be used, and are often inadequate to represent steeper loading variations [9].

This article presents novel stress and displacement solutions within a full-space under time-harmonic external loads. The full-space is a three-dimensional, homogeneous, isotropic, viscoelastic, unbounded medium. External time-harmonic loads are applied in the horizontal and vertical directions; bi-quadratic load distributions over a rectangular patch within the full-space are considered. The coupled Navier-Cauchy equations of motion describing this medium in the physical domain are solved by decomposing the displacement components into uncoupled potential and scalar fields and subsequent domain transformation through double Fourier transforms. This technique enables the original differential equations to be solved algebraically in the transformed domain. Transformed expressions for the external loads are obtained and then incorporated as boundary conditions in the transformed domain. Final expressions of stress and displacements within the full-space in the physical domain are written in terms of double improper integrals corresponding to double inverse Fourier transforms, which need to be evaluated numerically. These non-singular Green's functions can be used to model bounded and unbounded problems through boundary discretization and other meshless methods.

1.1 Problem statement

Consider a three-dimensional, isotropic full-space, described by Lame's constants μ and λ, damping coefficient η, and mass density ρ. In the absence of body forces, the Navier-Cauchy equations describing this medium are

$$\mu\nabla^2\boldsymbol{U} + (\lambda+\mu)\nabla(\nabla \bullet \boldsymbol{U}) = -\omega^2\rho\boldsymbol{U} \tag{1}$$

and

$$\sigma_{ij} = \lambda(\nabla \bullet \boldsymbol{U})\delta_{ij} + \mu(U_{i,j} + U_{j,i}). \tag{2}$$

in which $\boldsymbol{U}$ and $\boldsymbol{\sigma}$ are stress and displacement fields and ω is the frequency of excitation. This paper proposes to find solutions for $\boldsymbol{U}$ and $\boldsymbol{\sigma}$ for the cases in which the medium is under vertical and horizontal, bi-quadratically-distributed time-harmonic loads. Loads are applied over a rectangular area of sides $2A$ ($x-$direction) and $2B$ ($y-$direction), on the $x-y$ ($z=0$) plane (Fig. 1).

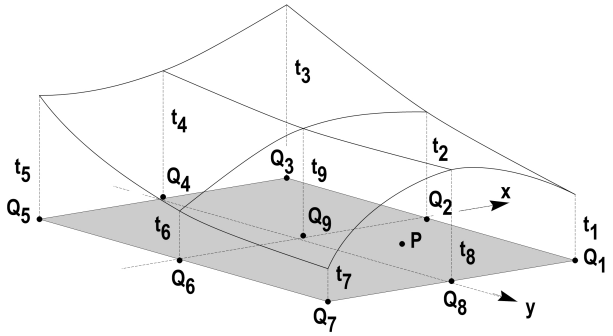

Figure 1. External loads with bi-quadratic distribution applied within the full-space.

2 General solution

According to Sommerfeld's radiation condition in this unbounded full-space [10], physical quantities such as the displacement field $\boldsymbol{U} = u_i\hat{e}_i$ ($i = x, y, z$) are required to vanish for $\mathbf{x} \to \pm\infty$. This linear-elastic field may be expressed according to the Helmholtz decomposition as [11]:

$$u_i = -\frac{1}{k_L^2}\Delta_{,i} + \frac{2}{k_S^2}\mathrm{e}_{imn}\Omega_{n,m}, \tag{3}$$

in which $k_L^2 = \omega^2\rho/(\lambda+2\mu)$ and $k_S^2 = \omega^2\rho/\mu$ are primary and secondary wave numbers, respectively, and $\boldsymbol{\Delta}$ and $\boldsymbol{\Omega}$ are vector fields. Considering the full-space to be isotropic, the constitutive equation results in

$$\frac{\sigma_{ij}}{\mu} = \delta_{ij}\frac{1-2n^2}{n^2}\Delta - \frac{2}{k_L^2}\Delta_{,ij} + \frac{2}{k_S^2}\left(\mathrm{e}_{ikl}\Omega_{l,kj} + \mathrm{e}_{jkl}\Omega_{k,li}\right) \tag{4}$$

for the stress components, in which δ_{ij} is the Kroenecker delta and $n^2 = k_L^2/k_S^2$. Trial solutions for the vector fields $\boldsymbol{\Delta}$ and $\boldsymbol{\Omega}$ can be written for domains $m=1$ ($-\infty < z \leq 0$) and $m=2$ ($0 \leq z < +\infty$) in a way that satisfies Sommerfeld [10] for both domains:

$$\Delta^{(1)} = A^{(1)}k_L^2\mathrm{e}^{\alpha_L z + \mathrm{i}(\beta x+\gamma y)}, \tag{5}$$

$$\Omega_j^{(1)} = B_j^{(1)}k_S^2\mathrm{e}^{\alpha_S z + \mathrm{i}(\beta x+\gamma y)}, \tag{6}$$

$$\Delta^{(2)} = A^{(2)}k_L^2\mathrm{e}^{-\alpha_L z + \mathrm{i}(\beta x+\gamma y)}, \tag{7}$$

and

$$\Omega_j^{(2)} = B_j^{(2)}k_S^2\mathrm{e}^{-\alpha_S z + \mathrm{i}(\beta x+\gamma y)}. \tag{8}$$

The solution of the title problem is then rewritten in terms of finding arbitrary functions $A^{(m)}$ ($m=1,2$) and $B_n^{(m)}$ ($n=1,2,3$) for the present loading case (Fig. 1).

The vector fields $\mathbf{\Delta}$ and $\mathbf{\Omega}$ must be such that $\mathrm{e}_{ijk}\Delta_{k,j} = \mathbf{0}$ and $\frac{\partial}{\partial x_i}\left[\mathrm{e}_{imn}\Omega_{n,m}\right] = 0$ [11]. Considering Eqs. 5 to 8, this results in

$$\alpha_{L,S}^2 = \left(\beta^2 + \gamma^2\right) - k_{L,S}^2, \tag{9}$$

and

$$B_3^{(1,2)} = \frac{\mp \mathrm{i}}{\alpha_S}\left(\beta B_1 + \gamma B_2\right). \tag{10}$$

The bi-quadratic external load considered in this article can be written as

$$\begin{aligned}\bar{p}_j\left(x, y, z = 0\right) = \frac{1}{4A^2B^2}\left(T_1x^2y^2 + T_2Bx^2y + 2T_3B^2x^2 + T_4ABxy + T_5Axy^2 + 2T_6AB^2x + 2T_7A^2y^2\right.\\ \left. + 2T_8A^2By + 4T_9A^2B^2\right),\end{aligned} \tag{11}$$

where $T_1 = t_1 + t_3 + t_5 + t_7 + 4t_9 - 2\left(t_2 + t_4 + t_6 + t_8\right)$, $T_2 = t_1 + 2t_4 + t_7 - \left(t_3 + t_5 + 2t_8\right)$, $T_3 = t_2 + t_6 - 2t_9$, $T_4 = t_1 + t_5 - \left(t_3 + t_7\right)$, $T_5 = t_1 + t_3 + 2t_6 - \left(2t_2 + t_5 + t_7\right)$, $T_6 = t_2 - t_6$, $T_7 = t_4 + t_8 - 2t_9$, $T_8 = -t_4 + t_8$, and $T_9 = t_9$ anywhere within the loaded area ($|x| < A$ and $|y| < B$; $z = 0$) and zero otherwise. The corresponding expression in the transformed Fourier domain is given by

$$\bar{p}_j\left(\beta, \gamma\right) = -\frac{1}{2A^2B^2\pi\beta^3\gamma^3}\sum_{i=1}^{9}\bar{p}_{ij}, \tag{12}$$

in which

$$\begin{aligned}\frac{\bar{p}_{1j}}{T_1} = &\left(\beta^2A^2 - 2\right)\left(\gamma^2B^2 - 2\right)\sin\left(\beta A\right)\sin\left(\gamma B\right) + 2\beta\gamma\left(\beta^2A^2 - 2\right)\sin\left(\beta A\right)\cos\left(\gamma B\right)\\ &+ 2\beta A\left(\gamma^2B^2 - 2\right)\cos\left(\beta A\right)\sin\left(\gamma B\right) + 4AB\beta\gamma\cos\left(\beta A\right)\cos\left(\gamma B\right),\end{aligned}$$

$$\begin{aligned}\frac{\bar{p}_{2j}}{T_2\mathrm{i}\gamma B} = &-\left(\beta^2A^2 - 2\right)\sin\left(\beta A\right)\sin\left(\gamma B\right) + \beta\gamma\left(\beta^2A^2 - 2\right)\sin\left(\beta A\right)\cos\left(\gamma B\right)\\ &- 2\beta A\cos\left(\beta A\right)\sin\left(\gamma B\right) + 2AB\beta\gamma\cos\left(\beta A\right)\cos\left(\gamma B\right),\end{aligned}$$

$$\frac{\bar{p}_{3j}}{2T_3\beta^2\gamma^2} = \left(\beta^2A^2 - 2\right)\sin\left(\beta A\right)\sin\left(\gamma B\right) + 2A\beta\cos\left(\beta A\right)\sin\left(\gamma B\right),$$

$$\frac{\bar{p}_{4j}}{T_4AB\beta\gamma} = -\sin\left(\beta A\right)\sin\left(\gamma B\right) + \gamma B\sin\left(\beta A\right)\cos\left(\gamma B\right) + A\beta\cos\left(\beta A\right)\sin\left(\gamma B\right) - AB\beta\gamma\cos\left(\beta A\right)\cos\left(\gamma B\right),$$

$$\begin{aligned}\frac{\bar{p}_{5j}}{T_5\mathrm{i}A\beta} = &-\left(\gamma^2\beta^2 - 2\right)\sin\left(\beta A\right)\sin\left(\gamma B\right) - 2B\gamma\sin\left(\beta A\right)\cos\left(\gamma B\right)\\ &+ A\beta\left(\gamma^2\beta^2 - 2\right)\cos\left(\beta A\right)\sin\left(\gamma B\right) + 2AB\beta\gamma\cos\left(\beta A\right)\cos\left(\gamma B\right),\end{aligned}$$

$$\frac{\bar{p}_{6j}}{2T_6\mathrm{i}AB\beta^2\gamma^2} = -\beta\gamma\sin\left(\beta A\right)\sin\left(\gamma B\right) + AB\beta\gamma\cos\left(\beta A\right)\sin\left(\gamma B\right),$$

$$\frac{\bar{p}_{7j}}{2T_7A^2\beta^2} = \left(\gamma^2\beta^2 - 2\right)\sin\left(\beta A\right)\sin\left(\gamma B\right) + 2\beta\gamma\sin\left(\beta A\right)\cos\left(\gamma B\right),$$

$$\frac{\bar{p}_{8j}}{2T_8\mathrm{i}A^2B\beta^2\gamma} = -\sin\left(\beta A\right)\sin\left(\gamma B\right) + \beta\gamma\sin\left(\beta A\right)\cos\left(\gamma B\right),$$

$$\frac{\bar{p}_{9j}}{4T_8A^2B^2\beta^2\gamma^2} = \sin\left(\beta A\right)\sin\left(\gamma B\right).$$

The substitution of the loading function into the boundary conditions results in the displacement and stress fields in terms of the Fourier wavenumbers. Inverse Fourier transforms must be performed numerically over the resulting expressions in order to obtain these fields in the physical domain. This results in 6 displacement components and 18 stress components, the final expressions of which are too long to show in this paper. The reader may refer to Romanini et al. [12] to obtain these expressions. Equation 13 shows a selected example of the horizontal displacement ($x-$direction) due to vertical loads ($z-$direction):

$$
\begin{aligned}
\frac{u_{XZ}}{D_N}\frac{z}{|z|} = &-T_1\frac{A^3}{a_0^3}\int_0^\infty\left(\int_0^\infty F_1\frac{F_{\beta 1}}{k_\beta^2}s_{\beta x}dk_\beta\right)\frac{F_{\gamma 1}}{k_\gamma^3}c_{\gamma y}dk_\gamma \\
&+T_2\frac{A^2B}{a_0^2}\int_0^\infty\left(\int_0^\infty F_1\frac{F_{\beta 1}}{k_\beta^2}s_{\beta x}dk_\beta\right)\frac{F_{\gamma 2}}{k_\gamma^2}s_{\gamma y}dk_\gamma \\
&-T_3\frac{2AB^2}{a_0}\int_0^\infty\left(\int_0^\infty F_1\frac{F_{\beta 1}}{k_\beta^2}s_{\beta x}dk_\beta\right)\frac{s_{\gamma B}}{k_\gamma}c_{\gamma y}dk_\gamma \\
&+T_4\frac{A^2B}{a_0}\int_0^\infty\left(\int_0^\infty F_1\frac{F_{\beta 2}}{k_\beta}c_{\beta x}dk_\beta\right)\frac{F_{\gamma 2}}{k_\gamma^2}s_{\gamma y}dk_\gamma \\
&-T_5\frac{A^3}{a_0^2}\int_0^\infty\left(\int_0^\infty F_1\frac{F_{\beta 2}}{k_\beta}c_{\beta x}dk_\beta\right)\frac{F_{\gamma 1}}{k_\gamma^3}c_{\gamma y}dk_\gamma \\
&-T_6 2AB^2\int_0^\infty\left(\int_0^\infty F_1\frac{F_{\beta 2}}{k_\beta}c_{\beta x}dk_\beta\right)\frac{s_{\gamma B}}{k_\gamma}c_{\gamma y}dk_\gamma \\
&-T_7\frac{2A^3}{a_0}\int_0^\infty\left(\int_0^\infty F_1 s_{\beta A}s_{\beta x}dk_\beta\right)\frac{F_{\gamma 1}}{k_\gamma^3}c_{\gamma y}dk_\gamma \\
&+T_8 2A^2B\int_0^\infty\left(\int_0^\infty F_1 s_{\beta A}c_{\beta x}dk_\beta\right)\frac{F_{\gamma 2}}{k_\gamma^2}s_{\gamma y}dk_\gamma \\
&-T_9 4AB^2a_0\int_0^\infty\left(\int_0^\infty F_1 s_{\beta A}s_{\beta x}dk_\beta\right)\frac{s_{\gamma B}}{k_\gamma}c_{\gamma y}dk_\gamma,
\end{aligned}
\tag{13}
$$

in which $D_N = -\frac{\eta_r+\mathrm{i}\eta_i}{2\mu\pi^2B^2a_0^2}$, $s_{\beta x} = \sin\left(\frac{a_0}{A}k_\beta x\right)$, $s_{\gamma y} = \sin\left(\frac{a_0}{A}k_\gamma y\right)$, $s_{\beta A} = \sin\left(a_0 k_\beta\right)$, $s_{\gamma B} = \sin\left(a_0 b_0 k_\gamma\right)$, $c_{\beta x} = \cos\left(\frac{a_0}{A}k_\beta x\right)$, $c_{\gamma y} = \cos\left(\frac{a_0}{A}k_\gamma y\right)$, $c_{\beta A} = \cos\left(a_0 k_\beta\right)$, $c_{\gamma B} = \cos\left(a_0 b_0 k_\gamma\right)$, $b_0 = \frac{B}{A}$, $a_0 = A\omega\sqrt{\frac{\rho}{\mu}}$, $\bar{\alpha}_L^2 = \left(k_\beta^2+k_\gamma^2\right) - \frac{(k_L^*/k_S^*)^2}{\eta_r+\mathrm{i}\eta_i}$, $\bar{\alpha}_S^2 = \left(k_\beta^2+k_\gamma^2\right) - \frac{1}{\eta_r+\mathrm{i}\eta_i}$, $F_1 = \mathrm{e}^{-\frac{a_0}{A}\bar{\alpha}_L|z|} - e^{-\frac{a_0}{A}\bar{\alpha}_S|z|}$, $F_2 = \bar{\alpha}_L\bar{\alpha}_S\mathrm{e}^{-\frac{a_0}{A}\bar{\alpha}_L|z|} - \left(k_\beta^2+k_\gamma^2\right)e^{-\frac{a_0}{A}\bar{\alpha}_S|z|}$, $F_3 = \bar{\alpha}_S\mathrm{e}^{-\frac{a_0}{A}\bar{\alpha}_L|z|} - \bar{\alpha}_L e^{-\frac{a_0}{A}\bar{\alpha}_S|z|}$, $F_{4,5} = k_{\gamma,\beta}^2\bar{\alpha}_S\mathrm{e}^{-\frac{a_0}{A}\bar{\alpha}_L|z|} + \left(k_{\beta,\gamma}^2 - \bar{\alpha}_S^2\right)\bar{\alpha}_L e^{-\frac{a_0}{A}\bar{\alpha}_S|z|}$, $F_{\beta 1} = \left(a_0^2k_\beta^2 - 2\right)s_{\beta A} + 2a_0k_\beta c_{\beta A}$, $F_{\beta 2} = -s_{\beta A} + a_0k_\beta c_{\beta A}$, $F_{\gamma 1} = \left(b_0^2a_0^2k_\gamma^2 - 2\right)s_{\gamma B} + 2b_0a_0k_\gamma c_{\gamma B}$, and $F_{\gamma 2} = -s_{\gamma B} + b_0a_0k_\gamma c_{\gamma B}$.

3 Numerical evaluation

The evaluation of the final displacement and stress fields requires special attention. The integrand of these functions contain singularities corresponding to the wave numbers of the full-space, and an oscillatory-decaying tail 2, which cannot be integrated properly with methods that involve truncation of the integration interval. In this work, these integrals were evaluated with a combination of techniques. The first was the incorporation of a small damping factor η in the elastic constants according to the correspondence principle [13]. This causes the singularities to fall slightly out of the real integration path (Fig. 2a), which enables the nearly-singular integrand to be evaluated with an adaptive Gauss quadrature [14]. The oscillatory-decaying portion of the integrand is evaluated with an improved series extrapolation algorithm, which can predict the result of the integral without truncating the integration interval [15].

The results from the present implementation were thoroughly validated with limiting cases from the literature. For the sake of this comparison, a solution for uniformly distributed dynamic loads was obtained by integrating the Kelvin solution by Kitahara [16] over a rectangular $2A \times 2B$ patch. The resulting uniformly distributed load was compared with the present implementation by making $t_i = 1$. Comparisons with the classical Kelvin point-load problem [17] were also obtained by making A and B small. Comparisons with the dynamic 2D plane-strain solution by [18] were possible by making the ratio B/A large. The results showed excellent agreement with these sources. Additionally, the implementation was shown to be able to reproduce the boundary conditions, which can be verified by checking whether the stress components reproduce the shape of the external load near the loaded surfaces.

Figures 3 and 4 show selected numerical results from the present implementation. These show displacement and stress fields within the full space for $\mu = 1$, $\rho = 1$, $\nu = 0.25$, $A = B = 1$, $t_i = i$ $(i = 1, ..., 9)$, and $\eta = 0.01$. Results are presented in terms of the normalized frequency of excitation $a_0 = \omega A/c_S$, in which $c_S^2 = \mu/\rho$ is the propagating speed of the shear wave in the full-space.

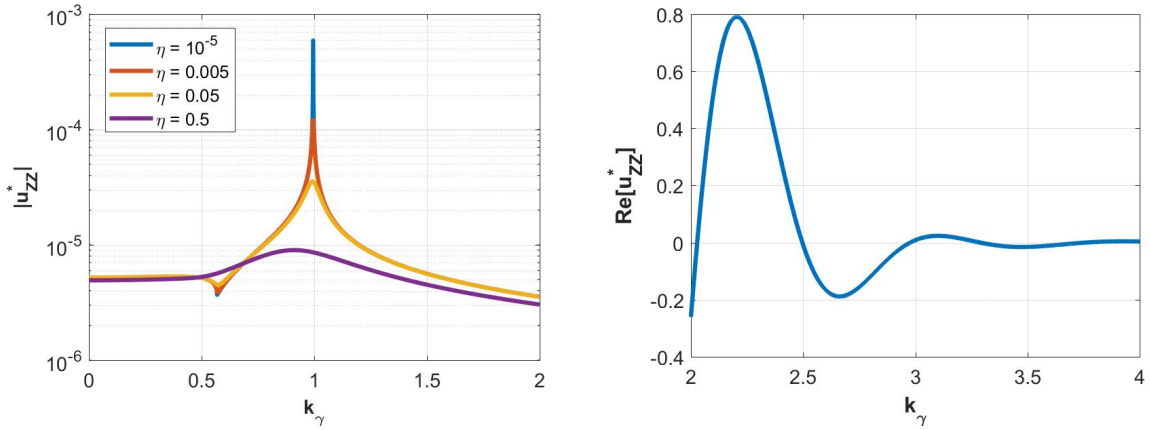

Figure 2. Selected example of integrand showing a) singular region and b) oscillatory-decaying region.

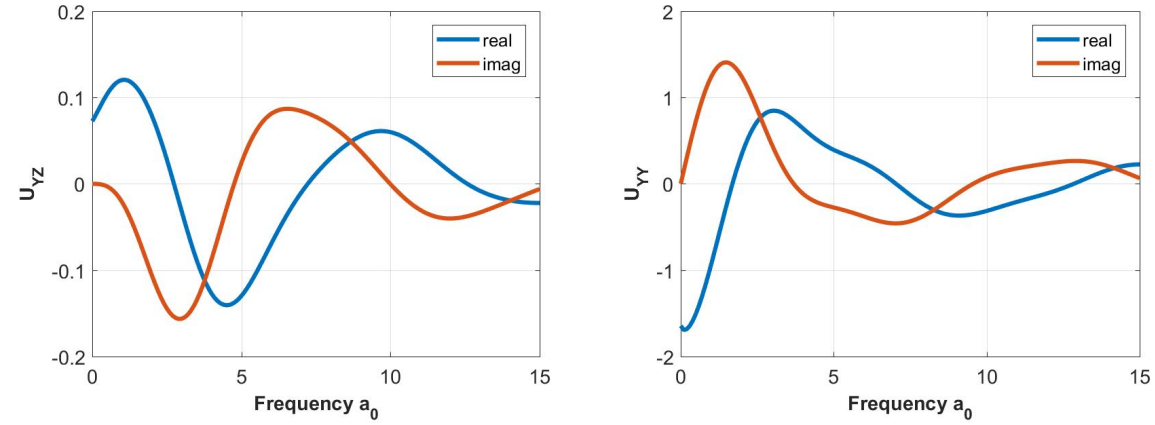

Figure 3. Selected displacement components.

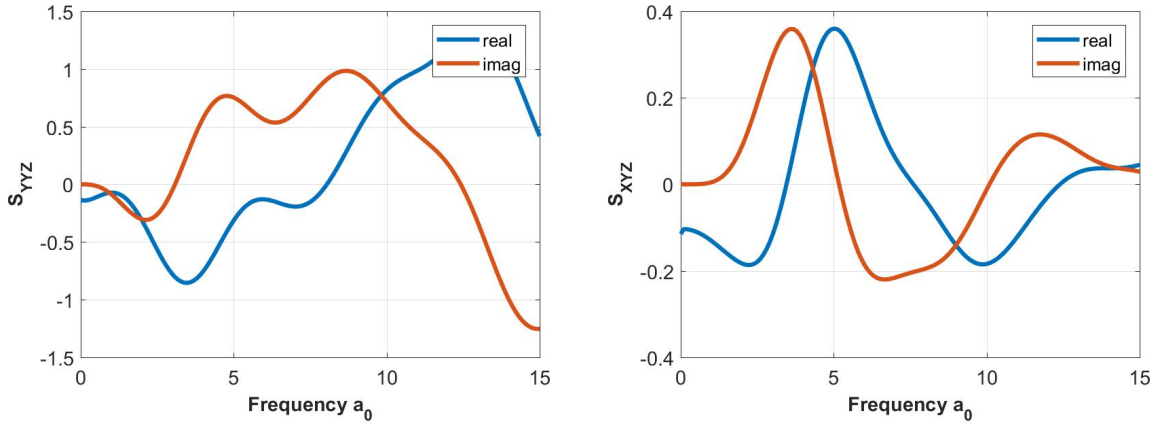

Figure 4. Selected stress components.

4 Conclusions

This paper introduced a new Green's function for isotropic homogeneous media. The differential equations describing the medium were solved with the aid of double Fourier transform, with which the originally coupled equations could be solved algebraically. A boundary-value problem corresponding to the case of bi-quadratically-distributed time-harmonic loads was considered. The paper presented strategies to evaluate the resulting double Fourier transforms, in which form the displacement and stress fields are expressed, and showed selected numerical results. The presented Green's function can be used as a bi-quadratic boundary element in elastodynamics.

Authorship statement. The authors hereby confirm that they are the sole liable persons responsible for the authorship of this work, and that all material that has been herein included as part of the present paper is either the property (and authorship) of the authors, or has the permission of the owners to be included here.

References

[1] R. He, A. M. Kaynia, and J. Zhang. A poroelastic solution for dynamics of laterally loaded offshore monopiles. *Ocean Engineering*, vol. 179, pp. 337–350, 2019.

[2] A. Galvis and P. Sollero. 2d analysis of intergranular dynamic crack propagation in polycrystalline materials a multiscale cohesive zone model and dual reciprocity boundary elements. *Computers & Structures*, vol. 164, pp. 1–14, 2016.

[3] R. Rodríguez, L. Moura, A. Galvis, E. Albuquerque, C.-L. Tan, and P. Sollero. Multi-scale dynamic failure analysis of 3d laminated composites using bem and mczm. *Engineering Analysis with Boundary Elements*, vol. 104, pp. 94–106, 2019.

[4] E. Mesquita, E. Romanini, and J. Labaki. Stationary dynamic displacement solutions for a rectangular load applied within a 3d viscoelastic isotropic full space – part i: Formulation. *Mathematical Problems in Engineering*, vol. 2012, 2012.

[5] J. Labaki, E. Romanini, and E. Mesquita. Stationary dynamic displacement solutions for a rectangular load applied within a 3d viscoelastic isotropic full space – part ii: Implementation, validation, and numerical results. *Mathematical Problems in Engineering*, vol. 2012, 2012.

[6] E. Romanini, J. Labaki, E. Mesquita, and R. Silva. Stationary dynamic stress solutions for a rectangular load applied within a 3d viscoelastic isotropic full-space. *Mathematical Problems in Engineering*, vol. 2019, 2019.

[7] E. Romanini, J. Labaki, A. Vasconcelos, and E. Mesquita. Influence functions for a 3d full-space under bilinear stationary loads. *Engineering Analysis with Boundary Elements*, vol. 130, pp. 286–299, 2021a.

[8] C. A. Brebbia and J. Dominguez. *Boundary elements: an introductory course*. WIT press, 1994.

[9] P. Barros and E. Mesquita. Singular-ended spline interpolation for two-dimensional boundary element analysis. *International Journal for Numerical Methods in Engineering*, vol. 47, n. 5, pp. 951–967, 2000.

[10] A. Sommerfeld. *Partial differential equations in physics*, volume 1. Academic press, 1949.

[11] H. Helmholtz. About integrals of hydrodynamic equations related with vortical motions. *J. für die reine Angewandte Mathematik*, vol. 55, pp. 25, 1858.

[12] E. Romanini, J. Labaki, I. Cavalcante, and E. Mesquita. A quadratic boundary element for 3d elastodynamics. *Engineering Analysis with Boundary Elements (submitted)*, vol. 132, pp. 1–2, 2021b.

[13] R. M. Christensen. *Theory of Viscoelasticity: Second Edition (Dover Civil and Mechanical Engineering)*. Dover Publications, 2010.

[14] R. Piessens, de E. Doncker-Kapenga, C. W. Überhuber, and D. K. Kahaner. *QUADPACK: a subroutine package for automatic integration*, volume 1. Springer Science & Business Media, 2012.

[15] P. Wynn. On a device for computing the e m (s n) transformation. *Mathematical Tables and Other Aids to Computation*, vol. 1, pp. 91–96, 1956.

[16] M. Kitahara. *Boundary integral equation methods in eigenvalue problems of elastodynamics and thin plates*. Elsevier, 2014.

[17] J. H. Kane. Boundary element analysis in engineering continuum mechanics(book). *Englewood Cliffs, NJ: Prentice Hall, 1994.*, vol. 1, 1994.

[18] P. Barros and E. Mesquita. Elastodynamic greens functions for orthotropic planestrain continua with inclined axes of symmetry. *International journal of solids and structures*, vol. 36, n. 31-32, pp. 4767–4788, 1999.